The development and origin of the two-stage silicification of Upper Jurassic limestones from the northern part of the Kraków-Częstochowa Upland (Southern Poland)

Alicja Kochman[1], Jacek Matyszkiewicz[2]

[1] AGH University of Krakow, Faculty of Geology, Geophysics and Environmental Protection, Krakow, Poland,
e-mail: kochman@agh.edu.pl (corresponding author), ORCID ID: 0000-0002-4003-6513
[2] AGH University of Krakow, Faculty of Geology, Geophysics and Environmental Protection, Krakow, Poland,
e-mail: jamat@agh.edu.pl, ORCID ID: 0000-0002-1812-9967

Abstract: The Upper Jurassic carbonates representing the microbial-sponge megafacies in the area of the Kraków-Częstochowa Upland (KCU) were locally silicified. In the reclaimed Lipówki Quarry, in Rudniki near Często-chowa (in the northern part of the Upland), macroscopically different silicification products were observed in blocks of Upper Jurassic limestones, deposited as mining waste. Two varieties were distinguished: (i) chert con-cretions representing the I silicification stage and (ii) light-brown, silicified limestones infilling the fractures in chert concretions or forming the cortices around the concretions or forming irregular bodies, all representing the II silicification stage. The diagnostic features are the following: (i) macroscopic development, (ii) the presence of moganite exclusively in chert concretions and (iii) significant differences in crystallinity index (CI) values, name-ly: 0.1–0.7 for chert concretions and 6.0–6.6 for silicified limestones. The formation of chert concretions was ini-tiated as early as in unconsolidated sediment, whereas the II silicification stage followed the chemical compaction of the limestones. The results of geochemical analyses of the products of both silicification stages indicated that the probable source of silica were the low-temperature hydrothermal solutions. Two types of fractures were found in the chert concretions, generated during different tectonic events. The older, open fractures were formed during the extension of the Late Jurassic sedimentary basin, which formerly occupied the territory of the more recent KCU. These fractures were infilled with unconsolidated, fine-detrital carbonate sediment, in which the concre-tions were embedded and finally silicified in the II silicification stage. The younger, closed fractures, transversal to those filled by the products of II silicification stage, along which small displacements are evident, document the later tectonic deformations presumably related to Cenozoic faulting.

Keywords: chert concretions, silicified limestones, stages of silicification, Upper Jurassic, tectonics, Kraków-Częstochowa Upland

INTRODUCTION

The Upper Jurassic carbonates from the Kraków-Częstochowa Upland (KCU) hosting silicifica-tion products represent the members of micro-bial-sponge megafacies, typical of the passive, northern margin of the Tethys Ocean (see e.g. Gwinner 1976, Gaillard 1983, Keupp et al. 1990, Leinfelder et al. 1994).

Exposures of these rocks are scattered along an extended belt which stretches from Portugal to the Caucasus Mts.

In the KCU, the Upper Jurassic microbial-sponge megafacies host siliceous sediments of diverse development and genesis (Kochman et al. 2020a, 2020b). The most common are chert concretions (Dżułyński 1951, Alexandrowicz 1960, Matyszkiewicz 1989, Świerczewska 1990), which usually accompany the bedded limestones, i.e. the sediments deposited onto the slopes of microbial-sponge carbonate buildups having the features of biostromes with an initial rigid framework (Matyszkiewicz 1997, cf. Pratt 1982). The bedded limestones belong to the so-called "normal facies" (Gwinner 1976) together with the platy limestones, which are the inter-bioherm sediments, devoid of chert concretions. In contrast, in the massive limestones which represent microbial-sponge buildups with a reticulate rigid framework, chert concretions are scarce. A particularly interesting variety of silicification products are the bedded cherts (Matyszkiewicz 1996), encountered somewhat rarely in the Upper Jurassic microbial-sponge megafacies and only observed in calciturbidites. Both the chert concretions and the bedded cherts are regarded as early diagenetic. The third type of silicification products includes epigenetic siliceous rocks (ESR), which reveal a significant variability in development and only occur in the topmost parts of the Upper Jurassic succession which have been preserved from erosion (Matyszkiewicz 1987, Matyszkiewicz et al. 2015, Kochman et al. 2020b).

The published descriptions available and the genetic models of silicification products found in the Upper Jurassic microbial-sponge megafacies, as well as in the other, similar carbonate facies of various ages, mainly concerned chert concretions (for details see e.g. Aldinger 1945, Dapples 1967, Beurer 1971, Knauth & Epstein 1976, Hein & Parrish 1987, Hesse 1989, Maliva & Siever 1989, Świerczewska 1990, 1997, Gao & Land 1991, Knauth 1992, Liedmann 1992, Lawrence 1994, Zhou et al. 1994, Reinhold 1996, Bustillo et al. 1998, Bolton et al. 1999, Beauchamp & Baud 2002, Sharp et al. 2002, Migaszewski et al. 2006, Wang et al. 2012, Neuweiler et al. 2014, Dong et al. 2018, Lin et al. 2018, Bourli et al. 2019, Lei et al. 2019, Yu et al. 2019, Abu-Mahfouz et al. 2023). In contrast, bedded cherts have received much less attention (e.g. Bustillo & Ruiz-Ortiz 1987, Świerczewska

1990, 1997, Matyszkiewicz 1996, Shen et al. 2018, Bourli et al. 2019, Kochman et al. 2020a, Matyszkiewicz & Kochman 2020). The development of microbial-sponge megafacies, when generalized throughout the area of their occurrence, have enabled researchers to construct genetic models applicable to the majority of the studied chert concretions and bedded cherts, whereas the origin of epigenetic silicification products (ESR) was typically controlled by local geological settings resulting from the geological history of particular regions, including tectonic events.

During mining operations conducted in the 20th century in several quarries in the northern part of the KCU (N-KCU), spectacular siliceous rocks were encountered and described by Premik (1937) and Wiśniewska-Żelichowska (1971). Unfortunately, these sediments are currently only accessible in the reclaimed Lipówki Quarry in Rudniki, located about 10 km to the northeast of Częstochowa (Fig. 1). The siliceous rocks can be observed in limestone blocks which were dumped during the quarrying as mining waste in the southwestern part of the lowest bench, at a point on the "Siliceous Valley" educational trail (Bąbelewska 2013, Bąbelewska et al. 2014). Apart from chert concretions, the limestone blocks also host porous, silicified limestone bodies of various shapes and sizes.

This publication presents the macro- and microscopic descriptions of siliceous deposits together with the microfacies development of limestones subjected to silicification. Finally, a trans-regional reconstruction has been attempted of the depositional conditions and relative ages of the products of both silicification stages, based upon the comparative studies made in both the southern and the northern parts of the KCU (S-KCU and N-KCU, respectively).

RESEARCH HISTORY

The silicification processes in the Upper Jurassic carbonates from the KCU have been studied since the early 19th century. However, that research focused on the mineralogical and petrographic features of chert concretions, which were of interest to both geologists and archaeologists (see Kochman et al. 2020a and references therein).

Following the macroscopic observations and mineralogical/petrographic studies, the genetic problems of both the chert concretions and the bedded cherts were discussed. Typically, the formation of chert concretions and bedded cherts during the early diagenetic silicification was widely accepted but the silicification mechanism and source of silica remained controversial. For the chert concretions, it was assumed that silicification proceeded on the slopes of microbial-sponge carbonate buildups and the sources of silica might have been the spicules of siliceous sponges (Matyszkiewicz 1997). In contrast, the origin of the bedded cherts was related to the silicification of calciturbidites (cf. Bustillo & Ruiz-Ortiz 1987, Matyszkiewicz 1996) and radiolarian shells were proposed as a possible silica source. Recently, observations have increasingly indicated the origin of silica from the sea-floor outflows of hydrothermal fluids genetically linked to the extensional tectonic events which took place between the Middle Oxfordian and the Early Kimmeridgian in the epicontinental basin located along the northern margin of the Tethys Ocean (Migaszewski et al. 2006, cf. Matyszkiewicz et al. 2015, Matyszkiewicz & Kochman 2020).

The secondary, epigenetic silicification of Upper Jurassic limestones became the subject of scientific interest as late as at the beginning of the 20th century (Kochman et al. 2020b and references therein). However, the origin of this process is still a matter of controversy. Three theories are generally discussed: (i) the action of hydrothermal solutions ascending along the faults or joint systems (Matyszkiewicz 1987, Matyszkiewicz et al. 2015, Matyszkiewicz & Kochman 2020), (ii) the weathering and erosion of Lower Cretaceous siliciclastic sediments preserved locally as covers resting upon the Upper Jurassic succession or infilling the fractures cutting through its carbonates (Bukowy 1960, Rajchel 1971, Heliasz 1980) or (iii) both (i) and (ii) processes operating together (Matyszkiewicz et al. 2015). However, the controversy not only concerns the source of the silica but also the age of silicification, which has been postulated to be: (i) the Early Cretaceous (Bukowy 1960, Rajchel 1971), (ii) the Cenozoic (Heliasz 1980), (iii) the Jurassic/Cretaceous turn (Górecka

& Zapaśnik 1981, Bednarek et al. 1983), (iv) the Early Cretaceous and the Cenozoic (Matyszkiewicz et al. 2015) and (v) only the Cenozoic (Kochman et al. 2020b).

The descriptions of early diagenetic and epigenetic siliceous deposits from the N-KCU are relatively scarce. Premik (1937, p. 14) described from the Rudniki Quarry the "huge, irregular, brownish, striped chert concretions", up to 3 m in diameter, hosted in the topmost part of massive limestones. The concretions were interconnected into an "almost continuous horizon". Their outer parts revealed significant porosity, which was interpreted by Premik (1937) as a result of the presence of calcium carbonate. Moreover, the same author also observed "small, irregular, black chert concretions" in massive limestones, which showed "sharp or almost indiscernible" contact with the overlying platy limestones (Premik 1937, p. 14).

Wiśniewska-Żelichowska (1971) described fossils from Upper Jurassic bioherms mined in several quarries in the Rudniki area, and found rather scarce chert nodules, up to a dozen centimeters across, hosted in limestone blocks. These were derived from bioherms, up to 9 meters thick, with uneven top and bottom surfaces. In one of these quarries, a horizon of huge chert concretions described by Premik (1937) was still accessible for observation.

In the Julianka area, located about 25 km east of Częstochowa, Heliasz (1980) found silicification features in chalky limestones representing the Idoceras planula zone, which locally graded into the massive or platy limestones. Silicification produced leaf-like cherts, up to about 0.8 meter thick, and elongated zones of silicified limestones, dozens of centimeters thick and several meters long. Moreover, Heliasz (1980) observed chert concretions in both the chalky and the silicified limestones. The cherts and the silicified limestones were composed of quartz accompanied by minor amounts of opal and chalcedony. Finally, Heliasz (1980) proposed the formation of silicified limestones to be later and their genesis to be different from those of the early diagenetic cherts. Moreover, he noticed that the epigenetic silicification is limited to the topmost part of Upper Jurassic succession and concluded that silica might have been

supplied via the solutions which infiltrated from the surface during the Tertiary.

The hydrothermal origin of the epigenetic silicified rocks (ESR) observed in the Upper Jurassic limestones from the central part of the KCU (C-KCU) was advanced by Górecka & Zapaśnik (1981) and Bednarek et al. (1983), basing upon measurements of the decrepitation temperatures of quartz. These authors also linked the ESR occurrences with the fault systems and determined the silicification age to be at the turn of the Jurassic/Cretaceous.

Silicification features from the Rudniki area were also described by Smoleńska (1983b), who found silicified zones up to 2.5 m thick and several dozen meters long in limestone bioherms. The zones were accompanied by two varieties of chert concretions: (i) chalky cherts and (ii) compact cherts. The inner parts of compact cherts were creamy or brownish-grey whereas the outer parts had white cortices, 1–2 cm thick, composed of chalky chert. Moreover, a difference in mineral composition was observed: the chalky cherts were composed of chalcedony and quartz whereas the compact cherts and the silicified zones were dominated by chalcedony.

The spectacular veins and crusts composed of the ESR were described by Matyszkiewicz et al. (2015) from fractures cutting through the Oxfordian limestones (Bifurcatus-Bimammatum zone) from Sokole Góry near Częstochowa (N-KCU). Based upon comprehensive mineralogical and petrographic observations, supported by geochemical and tectonic analyses, Matyszkiewicz et al. (2015) concluded the reaction of low-temperature hydrothermal solutions with the products of chemical weathering occurred during the two episodes of tectonic deformations: in the Valanginian and in the Cenozoic. In the veins, Matyszkiewicz et al. (2015) identified quartz with minor amounts of goethite, barite, galena and sphalerite. Chemical analyses revealed increased amounts of Pb and Cu.

Matyszkiewicz & Kochman (2020) demonstrated that the silicification products hosted in microbial-sponge megafacies from both the S-KCU and the N-KCU are considerably similar and closely related to the facies development of the enclosing Upper Jurassic sediments.

GEOLOGICAL SETTING

The Upper Jurassic carbonates from the N-KCU near Częstochowa represent almost full Oxfordian and the lower part of Kimmeridgian successions (Wierzbowski 1965, 1966, Trammer 1982, Matyja & Wierzbowski 2006). The monoclinal dipping of the Upper Jurassic strata to the northeast results in the appearance to the east of increasingly younger carbonate sediments showing significant facies diversity (Kutek et al. 1977, Matyja & Wierzbowski 2006). Matyja & Wierzbowski (2004) identified the Upper Jurassic sediments exposed on the surface in that area as the latitudinally extended Rudniki Biohermal Complex. Taking into account the short distance (about 3 km) from the Latosówka Quarry (Fig. 1) where the stratigraphic position of the sediments had already been documented by Matyja & Wierzbowski (2006), as well as the lack of major faults between the quarries, it can be suggested that the Upper Jurassic sediments encountered in the Lipówki Quarry also belong to the Idoceras planula zone. This theory was presented earlier by Różycki (1960), Wierzbowski (1965, 1966) and Wiśniewska-Żelichowska (1971).

In the area of Rudniki, Upper Jurassic limestones have been extracted since the mid-19th century and described by: Roemer (1870), Koronevich & Rebinder (1913), Premik (1930, 1934, 1937), Wiśniewska-Żelichowska (1932, 1971), Różycki (1953, 1960), Wierzbowski (1965, 1966), Smoleńska (1983a, 1983b) and Czop et al. (2009). Currently, in the hardly accessible, southeastern wall of the Lipówki Quarry in Rudniki, a 30-meter long succession of platy limestones is exposed. Moreover, in the southwestern wall of that quarry, the bedding of platy limestones disappears, and the limestone is composed of irregular clots dozens of centimeters across, with single, randomly distributed irregular chert concretions of diameters of up to 20 cm. Spectacular silicification products are observed in the Upper Jurassic limestone blocks, with volumes of up to several cubic meters piled in the southwestern part of the lowest bench (Fig. 2). Originally, these blocks were mining waste and were dumped in various parts of the lowest quarry bench during the operations of the Lipówki Quarry (closed in 1989).
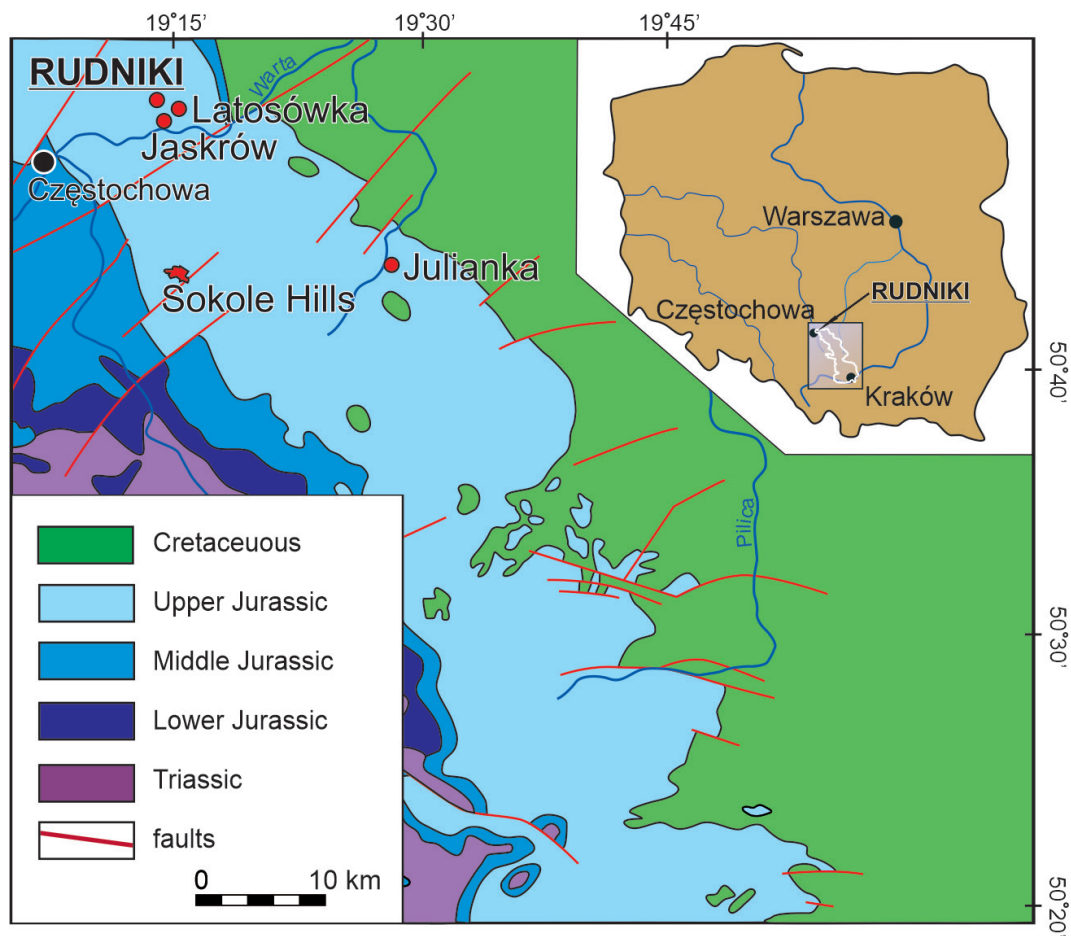
Fig. 1. *Location of the Rudniki area on the geological map of Poland (Rühle et al. 1977, simplified)*

Fig. 2. *Dump of Upper Jurassic limestone blocks with chert concretions and silicified limestones fragments in the reclaimed Lipówki Quarry, in Rudniki*

METHODS

From the deposited Upper Jurassic limestone blocks, a total of 25 samples were collected, including 10 samples of chert concretions and 10 of silicified limestones. Field observations were supported by photographic documentation of the sampling sites. Polished sections were prepared from all of the samples. Additionally, 11 thin sections were made and subjected to microscopic examination with an Olympus SZX10 polarizing microscope.

The principal research methods were microfacies analysis and petrographic studies. For the description of the SiO_2 phases, the simplified terminology was applied after Folk & Pittman (1971) and Klein & Hurlbut (1985), in which chalcedony, lutecite, quarzine and microflamboyant quartz (=flamboyant lutecite) were ascribed to a group of fibrous SiO_2 varieties. In this group, moganite (microcrystalline SiO_2 polymorph) was identified with the X-ray diffractometry (cf. Flörke et al. 1984, Miehe et al. 1984, Grätsch & Grünberg 2012, Zhang & Moxon 2014). Petrographic examinations revealed the presence of: (i) microcrystalline quartz (crystals <4 µm in diameter), microquartz (crystals between 4–20 µm in diameter) and megaquartz (crystals over 20 µm in diameter).

The X-ray powder diffraction analysis was carried on for 8 samples (4 of chert concretions and 4 of silicified limestones) in order to determine their mineral composition and crystallinity index (CI).

The samples were analysed at the Laboratory of Phase, Structural, Textural and Geochemical Analyses of the Faculty of Geology, Geophysics and Environmental Protection, AGH University of Krakow. The Rigaku SmartLab diffractometer operated under the following analytical conditions: graphite-monochromatized $Cu_{K\alpha}$ radiation (voltage: 45 kV, current: 200 mA), step 0.05° 2Θ, counting rate 1 s/step. The identification of mineral phases was based upon the interplanar spacings determined from diffractograms using the ICDD (2014) catalogue of diffraction data and the XRAYAN software. The CI of quartz was determined in accordance with the procedure described by Murata & Norman (1976).

The same samples were analyzed for the composition of major, REEs, and trace elements at Activation Laboratories Ltd. (ACTLABS) in Ancaster (Canada), using the fusion-inductively coupled plasma (FUS-ICP) and the fusion-inductively coupled plasma-mass spectrometry (FUS-MS) methodologies.

The Ce, Eu and Pr anomalies were determined with the methodology after Dulski (1994), and Bau & Dulski (1996). Anomalies were calculated from the following formulae: $Ce/Ce^* = Ce_{SN}/(0.5La_{SN} + 0.5Pr_{SN})$, $Eu/Eu^* = 3Eu_{SN}/(2Sm_{SN} + Tb_{SN})$ and $Pr/Pr^* = Pr_{SN}/(0.5Ce_{SN} + 0.5Nd_{SN})$ using the shale PAAS-normalized abundances (McLennan 1989, Piper & Bau 2013). The enrichment degree of light REEs (LREEs; La-Eu) relative to heavy REEs (HREEs; Gd-Yb) was presented as the ratio of shale-normalized La to Yb contents (La_{SN}/Yb_{SN}). The REE ratios and enrichments, especially $LREE_{SN}/HREE_{SN}$, La_{SN}/Yb_{SN}, La_{SN}/Sm_{SN}, Sm_{SN}/Yb_{SN}, were computed after Migaszewski et al. (2016).

MACROSCOPIC DESCRIPTION

The siliceous deposits are represented by chert concretions and silicified limestones. The chert concretions are elliptical or spherical (Figs. 3A, C, D, 4A) but also common are irregular shapes (Figs. 3B, 4B). Diameters reach up to 30 centimeters although concretions of up to 10 centimeters in size predominate. Some polished sections reveal concentric, banded structure of concretions (Fig. 5A, B). Occasionally, larger chert concretions are composed of several smaller nodules growing onto each other, with concentric bands developed in outer parts (Fig. 4B). Usually, chert concretions are various shades of brown or dark grey. In most specimens, the inner parts of the cherts are enveloped by bright or even white cortices, up to about 2 centimeters thick (Figs. 3A, B, D, 4A, 5) but in many samples such rims are absent (Figs. 3C, 4B). Locally, rusty-brown Liesegang rings can be seen within the concretions (Fig. 4B). In some larger chert concretions, open fractures are visible, infilled with silicified limestone (Figs. 4B, 5C). Such fractures show millimeters-size displacements developed along cross-cutting, transversal, closed fractures (Fig. 5C).
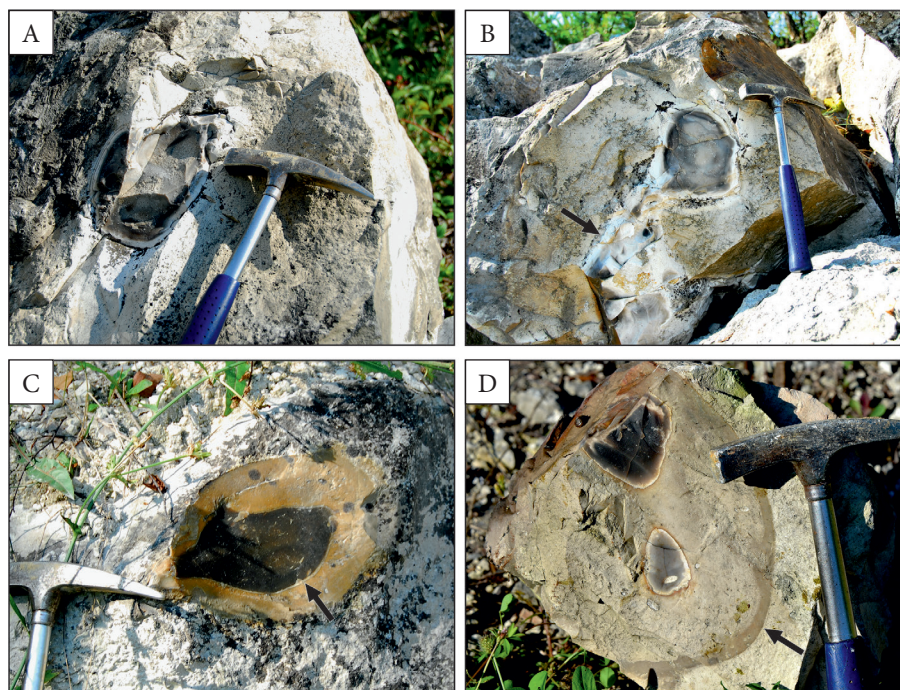
Fig. 3. *Macroscopic development of chert concretions and silicified limestones from the Lipówki Quarry: A) single, regular chert concretion enveloped by several-millimeters-thick white cortex; B) chert concretion composed of several interconnected bodies; to the left of spherical concretion its extension is visible as irregular body (arrow); white cortex enclosing the dark-grey nucleus has variable thickness; C) single, dark-brown concretion with light-brown envelope composed of silicified limestone; thin, white cortex is only locally present (arrow) at the boundary of chert concretion with silicified limestone; D) two chert concretions embedded within silicified limestone; siliceous sponge (arrow) affected by secondary silicification occurs at the boundary of silicified and unsilicified limestones*
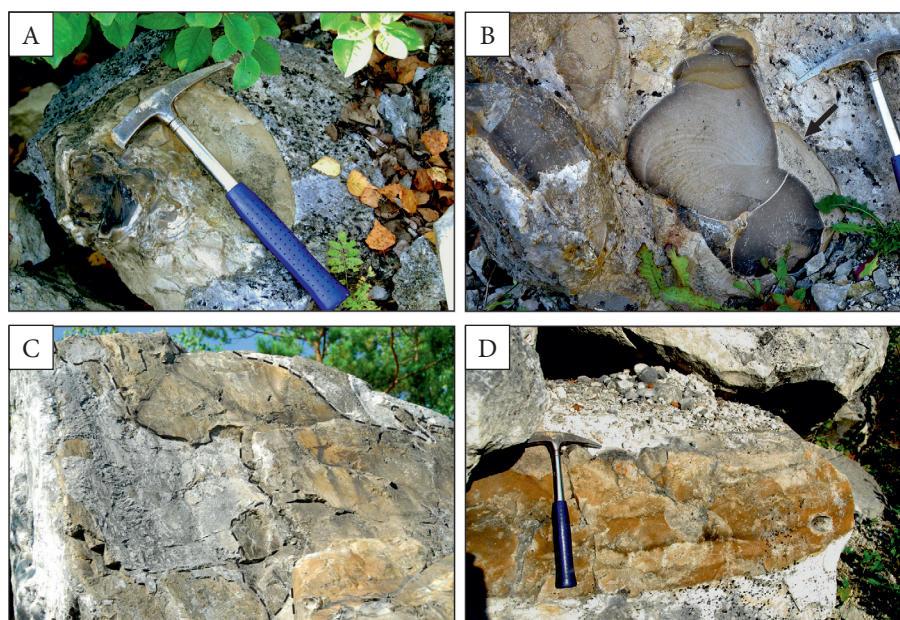

Fig. 4. *Macroscopic development of chert concretions and silicified limestones from the Rudniki Quarry: A) fractured chert concretion (left) enclosed by silicified limestone; B) chert concretion built of several bodies with banded structures (center); on the right (black arrow), silicified limestone is visible, which also infills a fracture in the chert concretion; in the upper part of chert concretion, rusty-brown Liesegang rings occur whereas on the left, an elongated, band-free concretion is present; C) silicified, irregularly shaped limestone fragment resting upon the joint surface; noteworthy is the complete absence of chert concretions; D) silicified limestone layer*
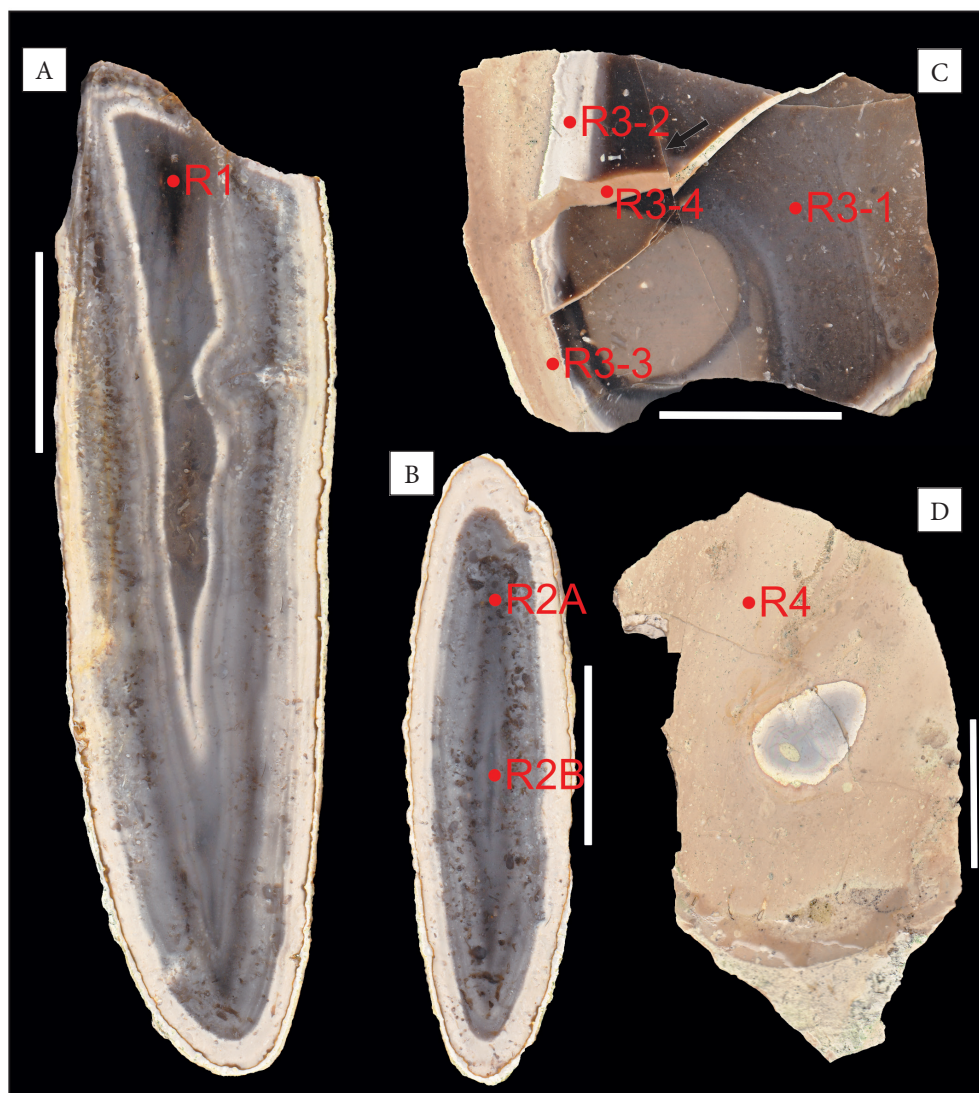
Fig. 5. *Polished sections of chert concretions and silicified limestones with marked sampling points for geochemical and X-ray analyses (see Tables 1, 2): A) and B) ellipsoidal, banded chert concretions (so-called onion structure); C) chert concretion on the right and in the center, on the left – fracture in chert concretion infilled by silicified limestone; the arrow marks the infilled and displaced fracture in chert concretion; D) chert concretion embedded within silicified limestone. Scale bars are 5 cm*

Silicified limestones are much more common than chert concretions. Three varieties were observed: (i) concentric cortices completely or partly enclosing the concretions, of thicknesses larger than diameters of the cherts (Figs. 3C, D, 4A, B, 5C, D), (ii) infillings of fractures in chert concretions, several millimeters thick (Figs. 4B, 5C), (iii) irregular bodies embedded within the limestones and covering areas of several square meters (Fig. 4C), and (iv) layers up to some tens of centimeters thick (Fig. 4D). Silicified limestones are light-brown and their boundaries with the enclosing, white, non-silicified limestones are sharp.

Another typical feature of the silicified limestones is their macroscopically visible porosity.

MICROSCOPIC DESCRIPTION

Chert concretions

The chert concretions are composed of several polymorphic varieties of SiO_2, mostly microcrystalline but also fibrous. Locally, micro- and megaquartz can also be present. In the completely silicified microcrystalline matrix, the relics of limestone components are seen, which can be filled with micro- or even megaquartz (Fig. 6A).
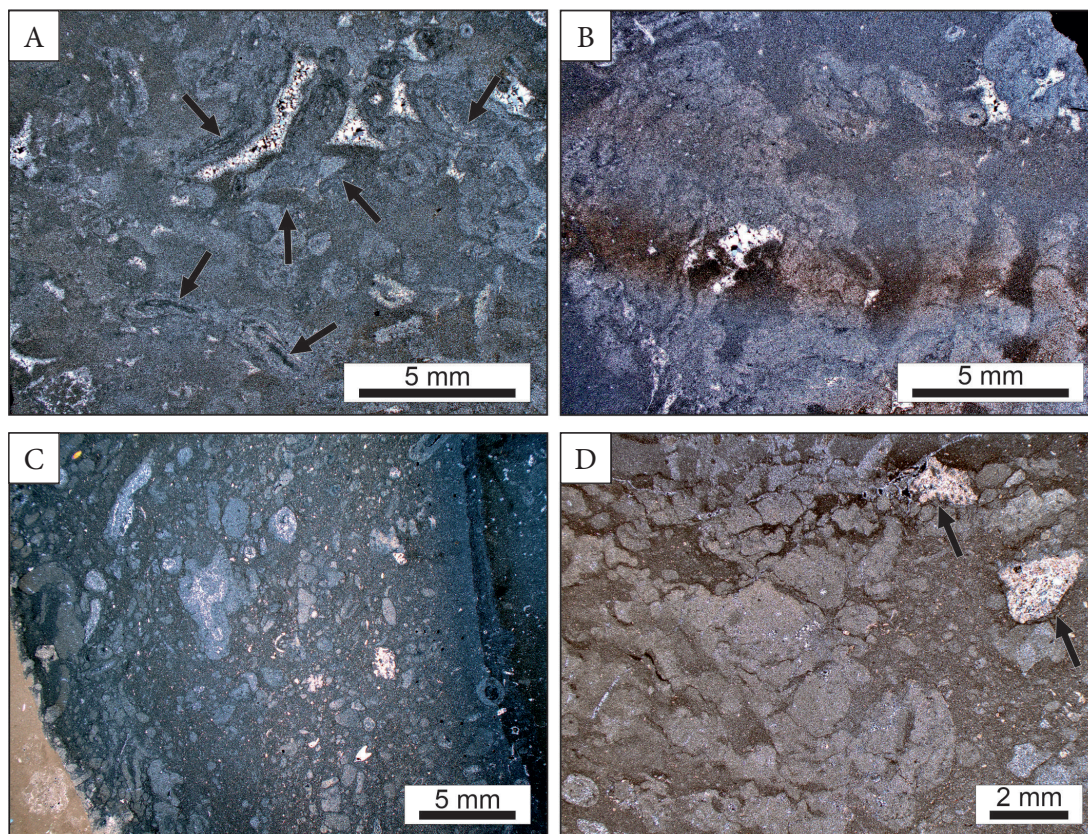
Fig. 6. *Microscopic images of chert concretions and silicified limestones under polarized light with crossed nicols: A) chert concretion with relics of silicified limestone (Crescientiella sp., arrows) and empty voids infilled with megaquartz; B) chert concretion with silicified columnar microbial stromatolites; larger voids are infilled with quartz and megaquartz in central part; the brown, horizontal band is the Liesegang ring; C) transitional zone from chert concretion (far right) to limestone (far left) developed as silicified limestone; in the chert concretion, larger relics of non-silicified limestone are absent, and the matrix is completely silicified; in the silicified limestone, both the matrix and some bioclasts are only partly replaced by silica; D) silicified limestone with pseudonodular texture composed of pseudonodules separated by dissolution seams. Larger bioclasts (arrows) are infilled with quartz with numerous calcite relics*

These are mostly bioclasts: spicules of siliceous sponges (monaxons and triaxons), fragments of bivalves and brachiopods, small gastropods, benthic foraminifers, ophiuroid ossicles, serpules, ostracods and calcispheres. Moreover, *Crescientiella* sp. (Fig. 6A), tuberoids with preserved fragments of siliceous sponge skeletons, calcareous sponges, oncoids, intraclasts and microbial structures (including spectacular columnar stromatolites, Fig. 6B) are present. The silicified bioclasts perfectly reveal visible contours and are composed of fibrous SiO_2, microcrystalline quartz or even megaquartz in their central parts. Fine open voids of a maximum size of up to several millimeters, typical with a stromatolite rigid framework, are filled with fibrous quartz along the margins and with megaquartz in the centers (Fig. 6A).

Calcite relics can sometimes be present in coarse-crystalline quartz, which fills the relics of larger bioclasts. The transition from chert concretions to silicified limestones is gradual. Usually, in the marginal zones of concretions, bioclasts do not occur due to the complete replacement of carbonates with silica (Fig. 6C).

Silicified limestones

The microscopic features of the silicified limestones are similar to chert concretions but the main component of the silicified matrix is microquartz. The main difference is the uncomplete replacement of the matrix, which contains numerous relics of calcite. This gives a slightly brownish color when observed in thin sections under unpolarized light (Figs. 6C, D, 7).
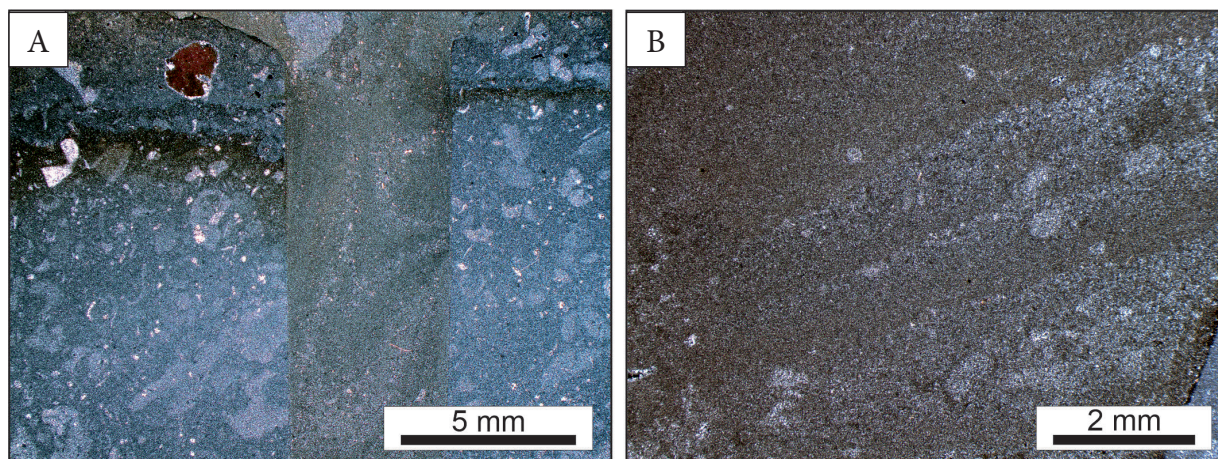
Fig. 7. *Microscopic images of fractures in chert concretions infilled with silicified limestones under polarized light and crossed nicols: A) silicified fracture (center) in chert concretion infilled with fine-detrital sediment showing relics of lamination; a boundary between the chert concretion and silicified limestone is evident in the upper part of photograph; B) laminated infilling of silicified fracture in chert concretion; fragment of boundary between silicified limestone and chert concretion is in the lower right corner*

Moreover, the matrix contains far more non-silicified relics of limestone components, rather scarce in chert concretions. On the contrary, the silicified limestones comprise pseudonodular textures with distinct dissolution seams (Fig. 6D), which are absent from the cherts. Silicified limestone, which infills the fractures in chert concretions, is a fine-grained, relatively well-sorted sediment of a wackestone-packstone character with evident relics of lamination (Fig. 7).

MAJOR AND TRACE ELEMENTS

The main component of all of the analyzed samples of chert concretions is SiO_2 (Table 1). Its contents vary from 95.61 to 98.02 wt.% (average: 96.53 wt.%). Other components are: Al_2O_3 – from 0.09 to 0.25 wt.% (average: 0.17 wt.%); Fe_2O_3 – from 1.23 to 1.77 wt.% (average: 1.49 wt.%) and MnO – from 0.011 to 0.017 wt.% (average: 0.014 wt.%). In the samples of silicified limestones (Table 1), contents of SiO_2 vary from 36.03 to 97.65 wt.% (average: 80.49 wt.%), those of Al_2O_3 – from 0.05 to 0.18 wt.% (average: 0.13 wt.%); Fe_2O_3 – from 0.06 to 1.60 wt.% (average: 0.92 wt.%) and MnO – from 0.010 to 0.014 wt.% (average 0.011 wt.%). The remaining elements show very low abundances except for a sample of the silicified infilling of a fracture in the chert concretion, which is clearly enriched with Cu (Table 1).

The La abundances, an indicator of REE sum variations (Chen et al. 2006), are generally low in both the chert concretions and the silicified limestones. Total REE contents are very low (<5 mg·kg⁻¹; Table 2). In all samples, the light REE (LREE) measured prevails over the heavy REE (HREE) with the LREE/HREE ratios varying from 4.16 to 19.36. The shale-normalized La_{SN}/Yb_{SN} ratios (mostly over 1; except for sample R1) confirm the relative enrichment of LREE *versus* HREE.

Because of a low number of samples subjected to lanthanide determinations and a high number of results below detection limits, REE anomalies should be interpreted with caution, especially in the case of heavy REE which show a high percentage of censored values.

RESULTS OF X-RAY DIFFRACTOMETRY

The X-ray diffractometry of the chert concretions reveals the presence of moganite and a crystallinity index (CI) from 0.1 to 0.7, which indicates low ordering of chalcedony structure (Table 3, Fig. 8). In the silicified limestones, the X-ray patterns confirm the presence of calcite and indicate the CI values from 6.0 to 6.6, which demonstrate much higher ordering of chalcedony structure in comparison with that from the concretions (Table 3, Fig. 8).

Table 1
Contents of major [wt.%] and trace [mg·kg⁻¹] elements in chert concretions and silicified limestones. Sample symbols are as in Figure 5

Sample	SiO_2	Al_2O_3	Fe_2O_3	MnO	MgO	CaO	Na_2O	K_2O	TiO_2	P_2O_5	LOI	Total	Ba	Rb	Sr	Pb	Th	U	Nb	Y	Zr	Ni	Co	Cu	Zn	Ga	Hf	V	Al/Al+Fe+Mn*
R1	95.61	0.25	1.68	0.017	0.01	0.08	0.05	0.02	0.014	<0.01	0.81	98.54	16	0.7	3.5	<0.5	0.14	0.1	1.3	0.2	7	5.4	0.9	7.9	3	0.50	<0.1	3	0.13
R2A	96.25	0.24	1.29	0.012	0.01	0.1	0.04	0.02	0.029	<0.01	0.97	98.96	13	0.5	3.2	<0.5	0.30	0.2	1.4	0.2	12	4.2	0.6	5.2	2	0.48	0.2	3	0.16
R2B	96.24	0.12	1.77	0.016	<0.01	0.09	0.05	0.01	0.029	0.02	0.72	99.07	4	0.3	2.8	0.5	0.30	0.4	1.1	1.0	10	4.6	0.9	5.2	4	0.68	0.2	2	0.06
R3-1	98.02	0.09	1.23	0.011	<0.01	0.09	0.04	0.01	0.003	<0.01	0.77	100.30	2	0.3	1.1	<0.5	0.06	0.2	0.3	0.2	3	3.3	0.5	4.1	<2	0.39	<0.1	2	0.07
R3-2	94.05	0.18	0.98	0.010	0.04	3.44	0.04	0.03	0.002	<0.01	2.07	100.80	11	0.6	21.8	<0.5	0.04	0.2	0.2	0.9	3	3.8	0.6	4.2	5	0.11	<0.1	1	0.15
R3-3	36.03	0.05	0.06	0.009	0.21	35.76	0.02	<0.01	0.002	0.02	28.27	100.40	5	0.5	102	<0.5	0.03	0.4	<0.2	3.5	2	<0.2	<0.1	0.6	6	<0.05	<0.1	3	0.42
R3-4	97.65	0.16	1.60	0.014	0.02	0.49	0.05	0.02	0.003	<0.01	0.34	100.03	7	0.5	2.4	0.9	0.03	0.1	0.3	0.7	2	5.7	0.8	30.1	7	0.27	<0.1	2	0.09
R4	94.22	0.13	1.05	0.011	0.03	2.14	0.03	0.02	0.011	0.03	1.53	99.20	14	0.4	14.1	<0.5	0.14	0.2	0.4	0.9	5	4.1	0.7	3.2	3	0.33	<0.1	1	0.11

* Al/Al+Fe+Mn – $Al_2O_3/Al_2O_3 + Fe_2O_3 + MnO$

Table 2
Contents of REE [mg·kg⁻¹] in chert concretions and silicified limestones. Sample symbols are as in Figure 5

| Sample	La	Ce	Pr	Nd	Sm	Eu	Gd	Tb	Dy	Ho	Er	Tm	Yb	Lu	LREE/HREE	La_{SN}/Yb_{SN}	La_{SN}/Sm_{SN}	Sm_{SN}/Yb_{SN}	Ce/Ce*	Pr/Pr*	Eu/Eu*
R1	0.20	0.35	0.04	0.13	0.04	0.008	0.03	<0.01	0.02	<0.01	0.01	<0.005	0.02	<0.002	9.60	0.74	0.73	1.02	0.90	1.10	–
R2A	0.38	0.74	0.09	0.31	0.06	0.008	0.04	<0.01	0.02	<0.01	0.01	<0.005	0.01	0.002	19.37	2.82	0.93	3.05	0.92	1.11	–
R2B	0.58	0.79	0.13	0.53	0.10	0.018	0.07	0.01	0.06	0.01	0.04	0.005	0.02	0.003	9.85	2.15	0.85	2.54	0.66	1.15	1.02
R3-1	0.23	0.30	0.04	0.11	0.02	<0.005	<0.01	<0.01	0.02	<0.01	0.01	<0.005	0.01	<0.002	17.50	1.71	1.68	1.02	0.71	1.29	–
R3-2	0.61	0.34	0.09	0.37	0.05	0.021	0.08	0.01	0.09	0.02	0.04	<0.005	0.01	<0.002	5.92	4.53	1.78	2.54	0.33	1.34	1.89
R3-3	2.07	0.60	0.23	0.94	0.19	0.047	0.25	0.04	0.29	0.06	0.17	0.023	0.13	0.017	4.16	1.18	1.59	0.74	0.19	1.48	1.09
R3-4	0.47	0.38	0.09	0.35	0.08	0.016	0.06	0.01	0.05	0.01	0.03	<0.005	0.02	<0.002	7.70	1.74	0.86	2.03	0.42	1.35	1.06
R4	0.62	0.52	0.11	0.47	0.11	0.022	0.11	0.01	0.08	0.01	0.04	0.006	0.03	<0.002	6.48	1.53	0.82	1.86	0.45	1.22	1.16
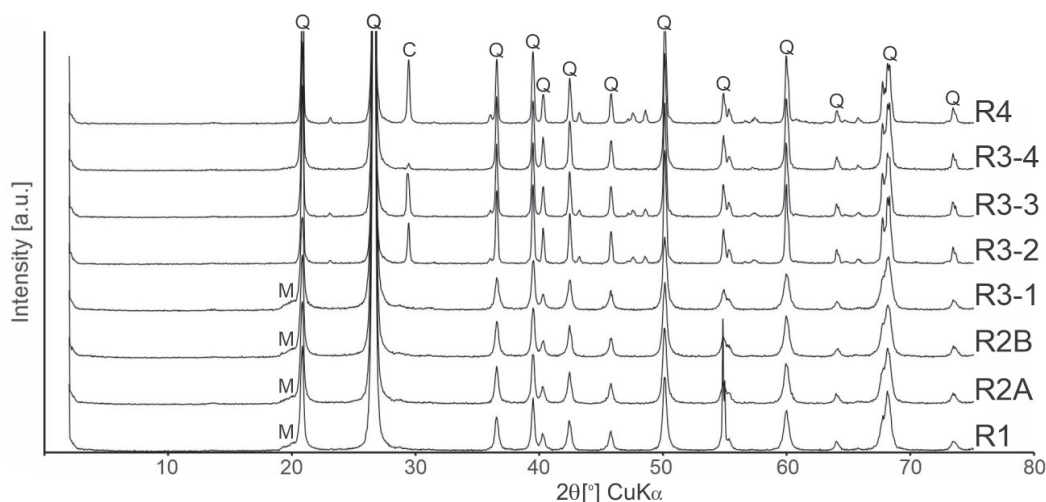
Fig. 8. *Examples of X-ray diffractograms of chert concretions (samples R1, R2A, R2B and R3-1) and silicified limestones (samples R3-2, R3-3, R3-4 and R4). Sample symbols, locations, and supplementary data as in Tables 1 and 2, and in Figure 5. Abbreviations: Q – quartz, M – moganite, C – calcite*

Table 3
Values of crystallinity index CI (after Murata & Norman 1976) in chert concretions and silicified limestones from Rudniki. Sample symbols are as in Figure 5

Sample	CI	CI-NM
R1	0.5	<1
R2	0.1	<1
R2B	0.7	<1
R3-1	0.2	<1
R3-2	6.6	6.6
R3-3	6.0	6.0
R3-4	6.2	6.2
R4	6.5	6.5

DISCUSSION AND CONCLUSIONS

The development of the siliceous deposits hosted in the Upper Jurassic limestones from the Lipów-ka Quarry allows us to draw a number of conclusions concerning not only the origin of sil: fication but also the evolution of the sedimentation and tectonics of the Upper Jurassic succession in the N-KCU.

Lithology of limestones

The lithology of the limestone facies hosting the silicification products in the Rudniki area corresponds to that described from the S-KCU by Dżułyński (1951) and Matyszkiewicz (1997). Chert concretions occur in limestones with an initial rigid framework formed by microbialites, siliceous sponges and *Crescientiella* sp. (cf. Krajewski & Olchowy 2023), which is typical of sediments laid down on the slopes of microbial-sponge carbonate buildups. This is documented by the presence of pseudonodular textures characteristic of an initial rigid framework from the peripheries of carbonate buildups subjected to chemical compaction (Matyszkiewicz & Kochman 2016).

Archival descriptions provided by Premik (1937), Wiśniewska-Żelichowska (1971) and Smoleńska (1983b) reveal that a typical feature of massive limestone bioherms from the Rudniki area is their considerable height in relation to lateral extent. This resulted in remarkable differences in the denivelation of the basin floor, additionally supported by a high susceptibility to the mechanical compaction of inter-biohermal sediments from which the platy limestones were finally formed (cf. Matyszkiewicz 1999, Kochman & Matyszkiewicz 2013, Matyszkiewicz & Kochman 2016). Such an interpretation is confirmed by the observations of Premik (1937, p. 15) who described carbonates from the Rudniki area as "slightly folded." Moreover, Wiśniewska-Żelichowska (1971, p. 9) stated that platy limestone layers have "distinct concavities and rise towards the bioherms."

Undoubtedly, such a varied morphology of the basin floor facilitated the generation of submarine mass movements, including calciturbidites, which were documented by Marcinowski (1970) in the adjacent Jaskrów Quarry (Fig. 2).

Progress of silicification

The first silicification stage presumably developed immediately after or even during the growth of the microbial-sponge carbonate buildups in unlithified sediments deposited onto the slopes of the buildups. This stage produced chert concretions, the typical features of which are: (i) the presence of moganite and (ii) the low ordering of chalcedony structure indicated by CI values <0.7. The formation of chert concretions proceeded during the very early burial diagenesis and was related to local redox-controlled boundaries (cf. Zijlstra 1987, Bourli et al. 2019). The initiation of concretions growth took place in the unlithified sediment, which was then subjected to extension. This resulted in the opening of fractures in poorly lithified concretions, then filled with the enclosing, fine-detrital, still unlithified carbonate sediment (Figs. 5C, 7). The extension of the Late Jurassic sedimentary basin at the turn of the Oxfordian/Kimmeridgian took place throughout the whole of the KCU and was confirmed by the presence of similar structures in the S-KCU (Fig. 9).
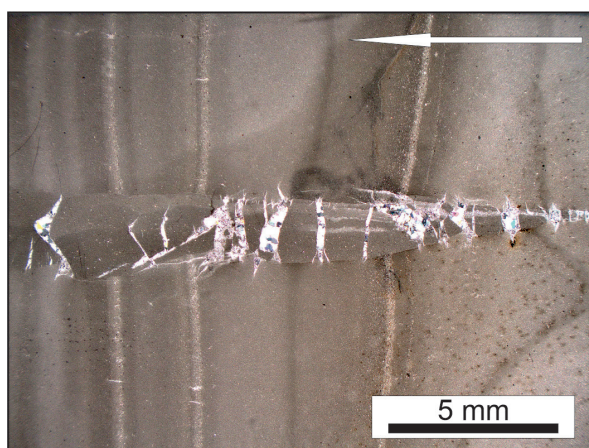

Fig. 9. *Carbonate infilling of the extensional fracture in calciturbidite, in which a bedded chert horizon was formed (outside the photograph). The arrow indicates the direction to the top. Sample from the S-KCU, turn of the Oxfordian/Kimmeridgian*

The second, much more extensive stage of silicification occurred after the completion of the early diagenesis of carbonate sediment and following its chemical compaction. It is indicated by the silicification of typical pseudonodular textures with distinct dissolution seams (Fig. 6D; Matyszkiewicz & Kochman 2016). The archival descriptions of Premik (1937), Wiśniewska-Żelichowska (1971) and Smoleńska (1983b) revealed a horizon of interconnected silica nodules, up to 3 meters thick, in the contact zone between the massive and platy limestones. It seems that this horizon corresponds to typical bedded cherts described in detail by Matyszkiewicz (1996) from calciturbidite successions in the S-KCU and found also in the N-KCU by Matyszkiewicz & Kochman (2020). The direct reason for the formation of thick chert horizons was the presence of stable redox boundaries in perfectly sorted calciturbidites (cf. Thomson et al. 1998, Bourli et al. 2019). The previously formed chert concretions were sometimes used as silica crystallization nuclei. At this stage, the open fractures cutting through the chert concretions and infilled with fine-detrital carbonate sediment were also silicified. If chert concretions were absent from the limestones, silicification invaded vast volumes of these carbonates. However, siliceous metasomatites formed under such conditions did not contain moganite and showed a much higher degree of the ordering of the chalcedony structure (CI = 6.0–6.6), corresponding to similar values reported from the S-KCU by Świerczewska (1997) and Kochman et al. (2020a).

Considering the enormous scale of II-stage silicification, the assumption of the biogenic origin of silica in bedded cherts hosted in calciturbidites from the KCU (Matyszkiewicz 1996, cf. Bustillo & Ruiz-Ortiz 1987) seems to be groundless. The most probable source of silica appears to be the solutions released from the sea-floor springs during trans-regional, extensional tectonic movements (Migaszewski et al. 2006).

The silica source proposed by Migaszewski et al. (2006) seems to be consistent with the growing number of results from detailed studies on the Upper Jurassic sediments from the KCU. In the S-KCU, Oxfordian neptunian dykes were observed, filled with quartz mineralization of a hydrothermal origin (formation temperatures close

to 90°C), which documented the Late Jurassic extensional tectonics (Matyszkiewicz et al. 2016). Moreover, the abundance of spicules of calcified siliceous sponges found in Upper Jurassic sediments did not correlate with the amount of chert concretions. In the Upper Jurassic succession from the S-KCU, the horizons were observed to be rich in calcified siliceous sponges and devoid of chert concretions together with those rich in chert concretions but poor in calcified siliceous sponges (Matyszkiewicz & Kochman 2016). Moreover, the encountered amounts of calcified siliceous sponges were far too low to be the sole or even the major source of SiO$_2$. Similarly, although noticed in the Upper Jurassic sediments from the KCU, radiolarians did not occur in that part of the relatively shallow, Late Jurassic sedimentary basin, in accumulations to have been a sufficient source of silica (cf. Bustillo & Ruiz-Ortiz 1987, Matyszkiewicz 1996). Therefore, the potential source of SiO$_2$ for chert concretions remains the hydrothermal solutions related to the episodes of Late Jurassic extensional tectonics in the KCU (cf. Matyszkiewicz et al. 2015, Kochman et al. 2020b).

The diagenesis might have changed SiO$_2$ contents in siliceous deposits (Geeslin & Chafetz 1982, Murray et al. 1992, Murray 1994), but Al, Ti, Fe and REE remained immobile during the diagenesis (Murray 1994). Taking into account the Al-Fe-Mn diagram (Adachi et al. 1986, Yamamoto 1987), it seems possible that hydrothermal solutions influenced the formation of both the chert concretions and the silicified limestones from Rudniki (Fig. 10).
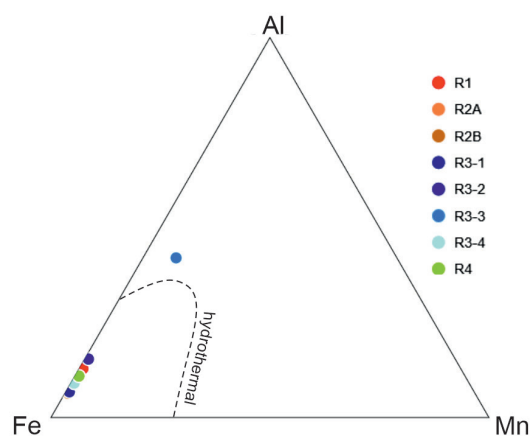

Fig. 10. *Al-Fe-Mn diagram for chert concretions and silicified limestones. Position of hydrothermal field after Adachi et al. (1986). Sample symbols as in Figure 5*

On the Al-Fe-Mn diagram, most samples fall into the field of hydrothermal activity, except for sample R3-3. The low values of geochemical parameter Al/Al+Fe+Mn seem to indicate the influence of a hydrothermal environment on the formation of siliceous precipitates (see e.g., Boström 1983, Sugisaki 1984, Adachi et al. 1986, Murray 1994, Wang et al. 2012). The Al/Al+Fe+Mn ratio depends on hydrothermal input to the sediments and decreases with the increasing intensity of hydrothermal activity, from 0.60 for biological deposition to 0.01 for hydrothermal precipitation (Adachi et al. 1986, Yamamoto 1987). The calculated values of Al/Al+Fe+Mn ratio vary from 0.16 to 0.06 for chert concretions and from 0.42 to 0.09 for silicified limestones.

Values below 0.6 are indicative of periodic influxes of fluids from hydrothermal vents into seawater (Adachi et al. 1986, Wang et al. 2012, Kochman et al. 2020b, Migaszewski et al. 2022). The contents of Ba, which is another indicator of hydrothermal activity (Halbach et al. 2002), vary from 0.0002 to 0.0016 wt.%. These values are much lower than those noticed in the Holy-Cross Mountains by Migaszewski et al. (2022).

The REE are applied as geochemical indicators of the influence of hydrothermal solutions on siliceous deposits (Michard 1989, German et al. 1990, Zhou et al. 1994, Chen et al. 2006). Due to the action of hydrothermal solutions, siliceous deposits inherit the REE patterns characterized by weak or no negative Ce anomalies and pronounced positive Eu anomalies. The negative Ce anomalies commonly result from the La enrichment of sediments affected by hydrothermal solutions (Bau & Dulski 1996, Yu et al. 2019). For chert concretions, the calculated Ce anomalies are negative and reach values of Ce/Ce* = 0.66–0.92 at Pr/Pr* = 1.10–1.29. For silicified limestones, the Ce anomalies are negative and show values of Ce/Ce* = 0.19–0.45 at Pr/Pr* = 1.22–1.48. Hence, the Ce anomalies are primary and are unrelated to enrichment in La. The Eu anomaly is another important indicator of the hydrothermal origin of cherts (Michard 1989, German et al. 1990, Zhou et al. 1994, Chen et al. 2006). The calculated Eu/Eu* ratios for silicified limestones vary from 1.06 to 1.89. It be stated that values of this ratio below 0.8 are indicative of negative anomalies whereas those above 1.2 point to positive

anomalies (Grawunder et al. 2014, Migaszewski et al. 2016). Moreover, the Eu/Eu* ratios over 1 suggest a strong contribution of hydrothermal solutions to silica deposition (Douville et al. 1999, He et al. 2019). Only a single sample R3-2 shows distinct, positive Eu anomaly. The general lack of clear positive Eu anomalies suggests that both the chert concretions and the silicified limestones might have formed from the waning hydrothermal solutions released at the end of hydrothermal activity in the distal parts of fracture systems, away from the main conduit zone, and/or with the increasing influence of seawater (German et al. 1990, Wang et al. 2012, He et al. 2019, Kochman et al. 2020b).

Summing up, the REE geochemical indicators: (i) strong LREE enrichments in relation to HREE, (ii) distinctly positive Eu and Pr anomalies and (iii) weak, negative to positive Ce anomalies, evidence the strong influence of hydrothermal events (German et al. 1990, 1999, Wang et al. 2012, Migaszewski et al. 2022). Variations of REE ratios and enrichments suggest the mixing of hydrothermal solutions and seawater during the formation of silica gel (German et al. 1990, 1999, Chen et al. 2006, Qiu & Wang 2011).

The final tectonic episode affecting the siliceous deposits from Rudniki was the formation of fractures transversal to those infilled with silicified limestone. Millimeters-long displacements along these fractures document another faulting episode of the Upper Jurassic sediments which followed the II stage of silicification and presumably took place in the Cenozoic.

REFERENCES

Abu-Mahfouz I.S., Cartwright J.A., Powell J.H., Abu-Mahfouz M.S., Olaf G. & Podlaha O.G., 2023. Diagenesis, compaction strain and deformation associated with chert and carbonate concretions in organic-rich marl and phosphorite; Upper Cretaceous to Eocene, Jordan. *Sedimentology*, 70(5), 1521–1552. https://doi.org/10.1111/sed.13085.

Adachi M., Yamamoto K. & Sugisaki R., 1986. Hydrothermal chert and associated siliceous rocks from the northern Pacific their geological significance as indication of ocean ridge activity. *Sedimentary Geology*, 47(1–2), 125–148. https://doi.org/10.1016/0037-0738(86)90075-8.

Aldinger H., 1945. Zur Stratigraphie des weißen Jura Delta in Württemberg. *Jahresberichte und Mitteilungen des Oberrheinischen Geologischen Vereins Band*, 31, 111–152. https://doi.org/10.1127/jmogv/31/1945/111.

Alexandrowicz S.W., 1960. Budowa geologiczna okolic Tyńca [Geological structure of the vicinity of Tyniec]. [in:] *Materiały do geologii obszaru śląsko-krakowskiego*, 5, Instytut Geologiczny – Biuletyn, 152, Wydawnictwa Geologiczne, Warszawa, 5–93.

Bau M. & Dulski P., 1996. Distribution of yttrium and rare-earth elements in the Penge and Kuruman iron-formations, Transvaal Supergroup, South Africa. *Precambrian Research*, 79(1–2), 37–55. https://doi.org/10.1016/0301-9268(95)00087-9.

Bąbelewska A., 2013. Porosty – mali pionierzy (stanowisko 9). [in:] Śliwińska-Wyrzychowska A. (red.), *Kopalnia przywrócona naturze: Przewodnik po przyrodniczej ścieżce dydaktyczno-edukacyjnej na obszarze nieczynnej kopalni odkrywkowej "Lipówka" w Rudnikach koło Częstochowy*, Agencja Wydawnicza "ARGI", Wrocław, 80–85.

Bąbelewska A., Musielińska R., Śliwińska-Wyrzychowska A., Bogdanowicz M. & Witkowska E., 2014. Edukacyjna rola nieczynnego kamieniołomu "Lipówka" w Rudnikach koło Częstochowy [The educational role of the "Lipówka" abandoned quarry in Rudniki near Częstochowa]. *Prace Komisji Krajobrazu Kulturowego PTG*, 26, 57–66.

Beauchamp B. & Baud A., 2002. Growth and demise of Permian biogenic chert along northwest Pangea: evidence for end-Permian collapse of thermohaline circulation. *Palaeogeography, Palaeoclimatology, Palaeoecology*, 184(1–2), 37–63. https://doi.org/10.1016/S0031-0182(02)00245-6.

Bednarek J., Górecka E. & Zapaśnik T., 1983. Uwarunkowanie tektoniczne rozwoju mineralizacji kruszcowej w utworach jurajskich monokliny śląsko-krakowskiej [Tectonically controlled development of ore mineralization in Jurassic sequence of the Silesian-Cracovian monocline]. *Annales Societatis Geologorum Poloniae*, 53(1–4), 43–62.

Beurer M., 1971. Kieselsäureanreicherungen in den oberjurasischen Sedimenten der Schwäbischen Alb. *Beihefte zum Geologischen Jahrbuch*, 69, 1–109.

Bolton E.W., Lasaga A.C. & Rye D.M., 1999. Long-term flow/chemistry feedback in a porous medium with heterogeneous permeability; kinetic control of dissolution and precipitation. *American Journal of Science*, 299(1), 1–68. https://doi.org/10.2475/ajs.299.1.1.

Boström K., 1983. Genesis of ferromanganese deposits-diagnostic criteria for recent and old deposits. [in:] Rona P.A., Boström K., Laubier L. & Smith K.L. (eds.), *Hydrothermal Processes at Seafloor Spreading Centers*, Plenum Press, New York, 473–483.

Bourli N., Kokkaliari M., Iliopoulos I., Pe-Piper G., Piper D.J., Maravelis A.G. & Zelilidis A., 2019. Mineralogy of siliceous concretions, cretaceous of Ionian zone, western Greece: implication for diagenesis and porosity. *Marine and Petroleum Geology*, 105, 45–63. https://doi.org/10.1016/j.marpetgeo.2019.04.011.

Bukowy S., 1960. Uwagi o sedymentacji i diagenezie albu okolic Krakowa. [in:] *Materiały do geologii obszaru śląsko-krakowskiego*, 5, Instytutu Geologiczny – Biuletyn, 152, Wydawnictwa Geologiczne, Warszawa, 243–276.

Bustillo M.Á. & Ruiz-Ortiz P.A., 1987. Chert occurrences in carbonate turbidites: Examples from the Upper Jurassic of the Betic Mountains (southern Spain). *Sedimentology*, 34(4), 611–621. https://doi.org/10.1111/j.1365-3091.1987.tb00790.x.

Bustillo M.Á., Delgado A., Rey J. & Ruiz-Ortiz P.A., 1998. Meteoric water participation in the genesis of Jurassic cherts in the Subbetic of southern Spain – a significant indicator of penecontemporaneous emergence. *Sedimentary Geology*, 119(1–2), 85–102. https://doi.org/10.1016/S0037-0738(98)00050-5.

Chen D., Hairou Q., Xin Y. & He L., 2006. Hydrothermal venting and basin evolution (Devonian, South China): Constraints from rare earth element geochemistry of chert. *Sedimentary Geology*, 183(3–4), 203–216. https://doi.org/10.1016/j.sedgeo.2005.09.020.

Czop M., Guzik M., Motyka J., Pacholewski A. & Różkowski K., 2009. Warunki hydrogeologiczne złoża wapieni i margli Latosówka-Rudniki w Rudnikach koło Częstochowy [Hydrogeological conditions of the Latosówka-Rudniki limestone and marl deposit in Rudniki near Częstochowa]. *Biuletyn Państwowego Instytutu Geologicznego*, 436(9/1), 69–75.

Dapples E.C., 1967. The diagenesis of sandstones. [in:] Larsen G. & Chilingar G.V. (eds.), *Diagenesis in Sediments*, Elsevier, Amsterdam, London, New York, 91–125.

Dong Y., He D., Sun S., Liu X., Zhou X., Zhang F., Yang Z. et al., 2018. Subduction and accretionary tectonics of the East Kunlun orogen, western segment of the Central China Orogenic System. *Earth-Science Reviews*, 186, 231–261. https://doi.org/10.1016/j.earscirev.2017.12.006.

Douville E., Bienvenu P., Charlou J.L., Donval J.P., Fouquet Y., Appriou P. & Gamo T., 1999. Yttrium and rare earth elements in fluids from various deep-sea hydrothermal systems. *Geochimica et Cosmochimica Acta*, 63(5), 627–643. https://doi.org/10.1016/S0016-7037(99)00024-1.

Dulski P., 1994. Interferences of oxide, hydroxide and chloride analyte species in the determination of rare earth elements in geological samples by inductively coupled plasmamass spectrometry. *Fresenius' Journal of Analytical Chemistry*, 350(4–5), 194–203. https://doi.org/10.1007/BF00322470.

Dżułyński S., 1951. Powstanie wapieni skalistych jury krakowskiej [The origin of the Upper Jurassic limestones in the Cracow area]. *Rocznik Polskiego Towarzystwa Geologicznego*, 21(2), 125–180.

Flörke O.W., Flörke U. & Giese U., 1984. Moganite, a new microcrystalline silica-mineral. *Neues Jahrbuch für Mineralogie Abhandlungen*, 149(3), 325–336.

Folk R.L. & Pittman J.S., 1971. Length-slow chalcedony: a new testament for vanished evaporites. *Journal of Sedimentary Research*, 41(4), 1045–1058. https://doi.org/10.1306/74D723F1-2B21-11D7-8648000102C1865D.

Gaillard C., 1983. Les biohermes à spongiaires et leur environment dans l'Oxfordian du Jura méridional. *Documents des Laboratoires de Géologie de la Faculté des Sciences de Lyon*, 90, 1–515.

Gao G.Q. & Land L.S., 1991. Nodular chert from the Arbuckle Group, Slick Hills, SW Oklahoma – a combined field, petrographic and isotopic study. *Sedimentology*, 38(5), 857–870. https://doi.org/10.1111/j.1365-3091.1991.tb01876.x.

Geeslin J.H. & Chafetz H.S., 1982. Ordovician Aleman ribbon cherts: An example of silicification prior to carbonate lithification. *Journal of Sedimentary Petrology*, 52(4), 1283–1293. https://doi.org/10.1306/212F811B-2B24-11D7-8648000102C1865D.

German C.R., Klinkhammer G.P., Edmond J.M., Mitra A. & Elderfield H., 1990. Hydrothermal scavenging of rare earth elements in the ocean. *Nature*, 345(6275), 516–518. https://doi.org/10.1038/345516a0.

German C.R., Hergt J., Palmer M.R. & Edmond J.M., 1999. Geochemistry of hydrothermal sediment core from the OBS vent field, 21°N East Pacific rise. *Chemical Geology*, 155(1–2), 65–75. https://doi.org/10.1016/S0009-2541(98)00141-7.

Górecka E. & Zapaśnik T., 1981. Dolomity epigenetyczne w utworach górnojurajskich monokliny śląsko-krakowskiej [Epigenetic dolomites in Upper Jurassic rocks in the Silesian-Cracow Monocline]. *Przegląd Geologiczny*, 29(10), 529–532.

Grawunder A., Merten D. & Büchel G., 2014. Origin of middle rare earth element enrichment in acid mine drainage-impacted areas. *Environmental Science and Pollution Research*, 21(11), 6812–6823. https://doi.org/10.1007/s11356-013-2107-x.

Grätsch H.A. & Grünberg J.M., 2012. Microstructure of flint and other chert raw materials. *Archaeometry*, 54(1), 18–36. https://doi.org/10.1111/j.1475-4754.2011.00610.x.

Gwinner M.P., 1976. *Origin of the Upper Jurassic Limestones of the Swabian Alb (Southern Germany)*. Contributions to Sedimentary Geology, 5, E. Schweizerbart, Stuttgart.

Halbach M., Halbach P. & Lüders V., 2002. Sulfide-impregnated and pure silica precipitates of hydrothermal origin from the Central Indian Ocean. *Chemical Geology*, 182(2–4), 357–375. https://doi.org/10.1016/S0009-2541(01)00323-0.

He J., Ding W., Huang W., Cao Z., Chen E., Dai P. & Zhang Y., 2019. Petrological, geochemical, and hydrothermal characteristics of Ordovician cherts in the southeastern Tarim Basin, NW China, and constraints on the origin of cherts and Permian tectonic evolution. *Journal of Asian Earth Sciences*, 170, 294–315. https://doi.org/10.1016/j.jseaes.2018.10.030.

Hein J.R. & Parrish J.T., 1987. Distribution of siliceous deposits in space and time. [in:] Hein J.R. (ed.), *Siliceous Sedimentary Rock-hosted Ores and Petroleum*, Van Nostrand Reinhold Co., New York, 10–57.

Heliasz Z., 1980. Sylifikacja wapieni w okolicach Julianki koło Częstochowy [Limestones silicifications in the Julianka area, near Częstochowa]. *Prace Naukowe Uniwersytetu Śląskiego w Katowicach*, 383, *Geologia*, 4, 92–101.

Hesse R., 1989. Silica diagenesis: origin of inorganic and replacement cherts. *Journal of Geology*, 26(1–3), 253–284. https://doi.org/10.1016/0012-8252(89)90024-X.

Keupp H., Koch R. & Leinfelder R., 1990. Steuerungsprozesse der Entwicklung von Oberjura-Spongiolithen Süddeutschlands: Kenntnisstand, Probleme und Perspektiven. *Facies*, 23, 141–174. https://doi.org/10.1007/BF02536711.

Klein C. & Hurlbut C.S., Jr., 1985. *Manual of Mineralogy (after James D. Dana)*. Wiley, New York.

Knauth L.P., 1992. Origin and diagenesis of cherts: An isotopic perspective. [in:] Clauer N. & Chaudhuri S. (eds.), *Isotopic Signatures and Sedimentary Records*, Lecture Notes in Earth Sciences, 43, Springer, Berlin, Heidelberg, 123–152. https://doi.org/10.1007/BFb0009863.

Knauth L.P. & Epstein S., 1976. Hydrogen and oxygen isotope ratios in nodular and bedded cherts. *Geochimica et Cosmochimica Acta*, 40(9), 1095–1108. https://doi.org/10.1016/0016-7037(76)90051-X.

Kochman A. & Matyszkiewicz J., 2013. Experimental method for estimation of compaction in the Oxfordian bedded limestones of the southern Kraków-Częstochowa Upland, Southern Poland. *Acta Geologica Polonica*, 63(4), 681–696. https://doi.org/10.2478/agp-2013-0029.

Kochman A., Matyszkiewicz J. & Wasilewski M., 2020a. Siliceous rocks from the southern part of the Kraków-Częstochowa Upland (Southern Poland) as potential raw materials in the manufacture of stone tools – a characterization and possibilities of identification. *Journal of Archaeological Science: Reports*, 30, 102195. https://doi.org/10.1016/j.jasrep.2020.102195.

Kochman A., Kozłowski A. & Matyszkiewicz J., 2020b. Epigenetic siliceous rocks from the southern part of the Kraków-Częstochowa Upland (Southern Poland) and their relation to Upper Jurassic early diagenetic chert concretions. *Sedimentary Geology*, 401, 105636. https://doi.org/10.1016/ j.sedgeo.2020.105636.

Koronevich P.M., Rebinder B.B., 1913. Geologicheskiye issledovaniya vdol' linii Gerby-Keletskoy zheleznoy dorogi na uchastke Gerby-Konetspol' v 1909-11 gg. *Izvestiya Geologicheskogo Komiteta*, 32, 938–1127 [Короневич П.М. & Ребиндер Б.Б., 1913. Геологические исследования вдоль линии Гербы-Келецкой железной дороги на участке Гербы-Конецполь в 1909-11 гг. *Известия Геологического Комитета*, 32, 938–1127].

Krajewski M. & Olchowy P., 2023. The role of the microencruster-microbial reef-building consortium in organic reefs evolution (Late Jurassic, northern Tethys shelf, southern Poland). *Facies*, 69, 4. https://doi.org/10.1007/s10347-023-00660-z.

Kutek J., Wierzbowski A., Bednarek J., Matyja B.A. & Zapaśnik T., 1977. Z problematyki stratygraficznej osadów górnojurajskich Jury Polskiej [Notes on the Upper Jurassic stratigraphy in the Polish Jura Chain]. *Przegląd Geologiczny*, 25(8–9), 438–445.

Lawrence M.J.F., 1994. Conceptual model for early diagenetic chert and dolomite, Amuri Limestone Group, north-eastern South Island, New Zeland. *Sedimentology*, 41(3), 479–498. https://doi.org/10.1111/j.1365-3091.1994.tb02007.x.

Lei Z., Dashtgard S., Wang J., Li M., Feng Q., Yu Q., Zhao A. & Du L., 2019. Origin of chert in Lower Silurian Longmaxi Formation: Implications for tectonic evolution of Yangtze Block, South China. *Palaeogeography, Palaeoclimatology, Palaeoecology*, 529(1), 53–66. https://doi.org/10.1016/j.palaeo.2019.05.017.

Leinfelder R.R., Krautter M., Laternser R., Nose M., Schmid D.U., Schweigert G., Werner W. et al., 1994. The origin of Jurassic reefs: Current research developments and results. *Facies*, 31, 1–56. https://doi.org/10.1007/BF02536932.

Liedmann W., 1992. *Diagenetische Entwicklung süddeutscher Malmkarbonate: unter Berücksichtigung lumineszenzpetrographischer, fluid inclusion und geochemischer Untersuchungsmethoden*. Universität, Heidelberg [PhD thesis, unpublished].

Lin L., Yu Y., Gao J. & Hong W., 2018. The origin and geochemical characteristics of Permian chert in the Eastern Sichuan Basin, China. *Carbonates and Evaporites*, 33(4), 613–624. https://doi.org/10.1007/s13146-017-0372-3.

Maliva R.G. & Siever R., 1989. Nodular chert formation in carbonate rocks. *Journal of Geology*, 97(4), 421–433. https://www.jstor.org/stable/30078348.

Marcinowski R., 1970. Turbidites in the Upper Oxfordian limestones at Jaskrów in the Polish Jura Chain. *Bulletin of the Polish Academy of Sciences, Earth Sciences*, 18(4), 219–225.

Matyja B.A. & Wierzbowski A., 2004. Stratygrafia i zróżnicowanie facjalne utworów górnej jury Wyżyny Krakowsko-Częstochowskiej i Wyżyny Wieluńskiej [Stratigraphy and facies development in the Upper Jurassic of the Kraków-Częstochowa Upland and the Wieluń Upland]. [in:] Partyka J. (red.), *Zróżnicowanie i przemiany środowiska przyrodniczo-kulturowego Wyżyny Krakowsko-Częstochowskiej. Tom 1: Przyroda*, Ojcowski Park Narodowy, Ojców, 13–26.

Matyja B.A. & Wierzbowski A., 2006. Julianka, coral colonization of the cyanobacteria-sponge bioherms at the turn of the Oxfordian and Kimmeridgian. [in:] Wierzbowski A., Aubrecht A., Golonka J., Gutowski J., Krobicki M., Matyja B.A., Pieńkowski G. & Uchman A. (eds.), *Jurassic of Poland and Adjacent Slovakian Carpathians: Field Trip Guidebook of 7th International Congress on the Jurassic System: Poland, Kraków, September 6–18, 2006*, Polish Geological Institute, Warszawa, 203–206.

Matyszkiewicz J., 1987. Epigenetic silification of the Upper Oxfordian limestones in the vicinity of Kraków. *Annales Societatis Geologorum Poloniae*, 57(1–2), 59–87.

Matyszkiewicz J., 1989. Sedimentation and diagenesis of the Upper Oxfordian cyanobacterial-sponge limestones in Piekary near Kraków. *Annales Societatis Geologorum Poloniae*, 59(1–2), 201–232.

Matyszkiewicz J., 1996. The significance of *Saccocoma*-calciturbidites for the analysis of the Polish epicontinental Late Jurassic Basin: An example from the Southern Cracow-Wielun Upland (Poland). *Facies*, 34, 23–40. https://doi.org/10.1007/BF02546155.

Matyszkiewicz J., 1997. *Microfacies, Sedimentation and Some Aspects of Diagenesis of Upper Jurassic Sediments from the Elevated Part of the Northern Peri-Tethyan Shelf: A Comparative Study on the Lochen Area (Schwäbische Alb) and the Cracow Area (Cracow-Wielun Upland, Polen)*. Berliner geowissenschaftliche Abhandlungen, E21, Selbstverlag Fachbereich Geowissenschaften, Berlin.

Matyszkiewicz J., 1999. Sea-bottom relief versus differential compaction in ancient platform carbonates: a critical reassessment of an example from Upper Jurassic of the Cracow-Wieluń Upland. *Annales Societatis Geologorum Poloniae*, 69(1–2), 63–79.

Matyszkiewicz J. & Kochman A., 2016. Pressure dissolution features in Oxfordian microbial-sponge buildups with pseudonodular texture, Kraków Upland, Poland. *Annales Societatis Geologorum Poloniae*, 86(4), 355–377. https://doi.org/10.14241/asgp.2016.008.

Matyszkiewicz J. & Kochman A., 2020. The provenance of siliceous rocks from the Kraków-Częstochowa Upland (Poland) used as raw-materials in the manufacture of siliceous artefacts from Central-Eastern Europe; An old problem in new light. *Journal of Archaeological Science: Reports*, 34(A), 102600. https://doi.org/10.1016/j.jasrep.2020.102600.

Matyszkiewicz J., Kochman A., Rzepa G., Gołębiowska B., Krajewski M., Gaidzik K. & Żaba J., 2015. Epigenetic silicification of the Upper Oxfordian limestones in the Sokole Hills (Kraków-Częstochowa Upland): relationship to facies development and tectonics. *Acta Geologica Polonica*, 65(2), 181–203. https://doi.org/10.1515/agp-2015-0007.

Matyszkiewicz J., Krajewski M., Kochman A., Kozłowski A. & Duliński M., 2016. Oxfordian neptunian dykes with brachiopods from the southern part of the Kraków-Częstochowa Upland (Southern Poland) and their links to hydrothermal vents. *Facies*, 62, 12. https://doi.org/10.1007/s10347-016-0464-x.

McLennan S.M., 1989. Rare earth elements in sedimentary rocks: influence of provenance and sedimentary processes. [in:] Lipin R. & McKay G.A. (eds.), *Geochemistry and Mineralogy of Rare Earth Elements*, Reviews in Mineralogy & Geochemistry, 21, De Gruyter, Berlin, Boston, 169–200. https://doi.org/10.1515/9781501509032-010.

Michard A., 1989. Rare earth element systematics in hydrothermal fluids. *Geochimica et Cosmochimica Acta*, 53(3), 745–750. https://doi.org/10.1016/ 0016-7037(89)90017-3.

Miehe G., Grätsch H. & Flörke O.W., 1984. Crystal structure and growth of fabric of length-fast chalcedony. *Physics and Chemistry of Minerals*, 10, 197–199. https://doi.org/10.1007/BF00309311.

Migaszewski Z.M., Gałuszka A., Durakiewicz T. & Starnawska E., 2006. Middle Oxfordian – Lower Kimmeridgian chert nodules in the Holy Cross Mountains, south-central Poland. *Sedimentary Geology*, 187(1), 11–28. https://doi.org/10.1016/j.sedgeo.2005.12.003.

Migaszewski Z.M., Gałuszka A. & Dołęgowska S., 2016. Rare earth and trace element signatures for assessing an impact of rock mining and processing on the environment: Wiśniówka case study, south-central Poland. *Environmental Science and Pollution Research*, 23(24), 24943–24959. https://doi.org/10.1007/s11356-016-7713-y.

Migaszewski Z.M., Gałuszka A. & Migaszewski A., 2022. Geochemistry and petrology of striped chert as a provenance tool for artefacts from the Krzemionki Neolithic mining area (Poland). *Archaeometry*, 64(5), 1093–1109. https://doi.org/10.1111/arcm.12778.

Murata K.J. & Norman M.B., 1976. An index of crystallinity for quartz. *American Journal of Science*, 276(9), 1120–1130. https://doi.org/10.2475/ ajs.276.9.1120.

Murray R.W., 1994. Chemical criteria to identify the depositional environment of chert: general principles and applications. *Sedimentary Geology*, 90(3–4), 213–232. https://doi.org/10.1016/0037-0738(94)90039-6.

Murray R.W., Buchholtz Ten Brink M.R., Gerlach D.C., Russ III G.P. & Jones D.L., 1992. Rare earth, major, and trace element composition of Monterey and DSDP chert and associated host sediment: assessing the influence of chemical fractionation during diagenesis. *Geochimica et Cosmochimica Acta*, 56(7), 2657–2671. https://doi.org/10.1016/0016-7037(92)90351-I.

Neuweiler F., Larmagnat S., Molson J. & Fortin-Morin F., 2014. Sponge spicules, silicification, and sequence stratigraphy. *Journal of Sedimentary Research*, 84(11), 1107–1119. https://doi.org/10.2110/jsr.2014.86.

Piper D.Z. & Bau M., 2013. Normalized rare earth elements in water, sediments, and wine: identifying sources and environmental redox conditions. *American Journal of Analytical Chemistry*, 4(10A), 69–83. https://doi.org/10.4236/ajac.2013.410A1009.

Pratt B.R., 1982. Stromatolitic framework of carbonate mud-mounds. *Journal of Sedimentary Petrology*, 52(4), 1203–1227. https://doi.org/10.1306/212F80FD-2B24-11D7-8648000102C1865D.

Premik J., 1930. Sprawozdanie z badań geologicznych, dokonanych w roku 1929 na obszarze Kłobucka-Wręczycy, Rudnik (na NE od Częstochowy) i nad środkową Widawką. *Posiedzenia Naukowe Państwowego Instytutu Geologicznego*, 25, 26–32.

Premik J., 1934. Budowa i dzieje geologiczne okolic Częstochowy. *Ziemia Częstochowska*, 1, 256–266.

Premik J., 1937. Sprawozdanie z badań geologicznych wykonanych w r. 1936 na arkuszu Częstochowa oraz Woźniki. *Posiedzenia Naukowe Państwowego Instytutu Geologicznego*, 47, 13–15.

Qiu Z. & Wang Q.C., 2011. Geochemical evidence for submarine hydrothermal origin of the Middle-Upper Permian chert in Laibin of Guangxi, China. *Science China Earth Sciences*, 54(7), 1011–1023. https://doi.org/10.1007/s11430-011-4198-x.

Rajchel J.M., 1971. Badania sedymentologiczne krzemieni jurajskich pod Krakowem. *Sprawozdania z Posiedzeń Komisji Naukowych Polskiej Akademii Nauk. Oddział w Krakowie*, 14(2), 625–645.

Reinhold C., 1996. *Prozesse, Steuerung und Produkte komplexer Diagenese-Sequenzen in süddeutschen Malm-Karbonaten*. Technische Universität, Berlin [PhD thesis, unpublished].

Roemer F., 1870. *Geologie von Oberschlesien*. Robert Nischkowsky, Breslau.

Różycki S.Z., 1953. *Górny dogger i dolny malm Jury Krakowsko-Częstochowskiej: (opis odsłonięć)*. Prace – Instytut Geologiczny, 17, Wydawnictwa Geologiczne, Warszawa.

Różycki S.Z., 1960. Czwartorzęd regionu Jury Krakowsko-Częstochowskiej i sąsiadujących z nią obszarów [Quaternary of the Częstochowa Jura Chain and the adjacent areas]. *Przegląd Geologiczny*, 8, 424–429.

Rühle E., Ciuk E., Osika R. & Znosko J., 1977. *Mapa geologiczna Polski bez utworów czwartorzędowych: 1:500 000 [Geological map of Poland without Quaternary formations, scale 1: 500 000]*. Wydawnictwa Geologiczne, Warszawa.

Sharp Z.D., Durakiewicz T., Migaszewski Z.M. & Atudorei V.N., 2002. Antiphase hydrogen and oxygen isotope periodicity in chert nodules. *Geochimica et Cosmochimica Acta*, 66(16), 2865–2973. https://doi.org/10.1016/S0016-7037(02)00873-6.

Shen B., Ma H., Ye H., Lang X., Pei H., Zhou C., Zhang S. & Yang R., 2018. Hydrothermal origin of syndepositional chert bands and nodules in the Mesoproterozoic Wumishan Formation: Implications for the evolution of Mesoproterozoic cratonic basin, North China. *Precambrian Research*, 310, 213–228. https://doi.org/10.1016/j.precamres.2018.03.007.

Smoleńska A., 1983a. Wykształcenie litologiczne górnojurajskich wapieni mikrytowych rejonów Działoszyna i Rudnik [Lithology of the Upper Jurassic micritic limestones region of Działoszyn and Rudniki]. *Zeszyty Naukowe AGH, Geologia*, 9(1), 39–66.

Smoleńska A., 1983b. Biohermowe wapienie gąbkowe okolic Częstochowy i Rudnik [Biohermal, spongy limestones from the vicinity of Częstochowa and Rudniki]. *Zeszyty Naukowe AGH, Geologia*, 9(3), 47–60.

Sugisaki R., 1984. Relation between chemical composition and sedimentation rate of Pacific Ocean-floor sediments deposited since the Middle Cretaceous: Basic evidence for chemical constraints on depositional environments of ancient sediments. *The Journal of Geology*, 92(3), 235–259. https://www.jstor.org/stable/30069398.

Świerczewska A., 1990. *Sylifikacja diagenetyczna w wapieniach jurajskich Jury Krakowsko-Wieluńskiej*. Polish Academy of Sciences, Warszawa [PhD thesis, unpublished].

Świerczewska A., 1997. Early diagenetic silicification in the Upper Jurassic biohermal and interbiohermal facies. [in:] Schild R. & Sulgostkowska Z. (eds.), *Man and flint: Proceedings of the VII*[th] *International Flint Symposium Warszawa – Ostrowiec Świętokrzyski, September 1995*, Institute of Archaeology and Ethnology Polish Academy of Sciences, Warszawa, 357–361.

Thomson J., Jarvis I., Green D.R.H., Green D.A. & Clayton T., 1998. Mobility and immobility of redox-sensitive elements in deep-sea turbidites during shallow burial. *Geochimica et Cosmochimica Acta*, 62(4), 643–656. https://doi.org/10.1016/S0016-7037(97)00378-5.

Trammer J., 1982. Lower to Middle Oxfordian sponges of the Polish Jura. *Acta Geologica Polonica*, 32, 1–39.

Wang J., Chen D., Wang D., Yan D., Zhou X. & Wang Q., 2012. Petrology and geochemistry of chert on the marginal zone of Yangtze Platform, western Hunan, South China, during the Ediacaran-Cambrian Transition. *Sedimentology*, 59(3), 809–829. https://doi.org/10.1111/j.1365-3091.2011.01280.x.

Wierzbowski A., 1965. Problem granicy oksford-kimeryd w północnej części Jury Krakowsko-Częstochowskiej. *Annales Societatis Geologorum Poloniae*, 35(2), 291–300.

Wierzbowski A., 1966. Górny oksford i dolny kimeryd Wyżyny Wieluńskiej. *Acta Geologica Polonica*, 16(2), 127–200.

Wiśniewska-Żelichowska M., 1932. Les Rhynchonellidés du Jurassique supérieur de Pologne. *Palaeontologia Polonica*, 2(1), 1–71.

Wiśniewska-Żelichowska M., 1971. Fauna bioherm jurajskich w Rudnikach pod Częstochową. [in:] *Z badań geologicznych regionu śląsko-krakowskiego*, 11, Biuletyn – Instytut Geologiczny, 243, Wydawnictwa Geologiczne, Warszawa, 5–63.

Yamamoto K., 1987. Geochemical characteristics and depositional environments of cherts and associated rocks in the Franciscan and Shimanto Terranes. *Sedimentary Geology*, 52(1–2), 65–108. https://doi.org/10.1016/0037-0738(87)90017-0.

Yu Y., Lin L., Deng X., Wang Y., Li Y. & Guo Y., 2019. Geochemical features of the Middle–Upper Permian cherts and implications for origin, depositional environment in the Sichuan Basin, SW China. *Geological Journal*, 55(2), 1493–1506. https://doi.org/10.1002/gj.3511.

Zhang M. & Moxon T., 2014. Infrared absorption spectroscopy of SiO_2-moganite. *American Mineralogist*, 99(4), 671–680. https://doi.org/10.2138/am.2014.4589.

Zhou Y., Chown E.H., Guha J., Lu H. & Tu G., 1994. Hydrothermal origin of Late Proterozoic bedded chert at Gusui, Guangdong, China: petrological and geochemical evidence. *Sedimentology*, 41(3), 605–619. https://doi.org/10.1111/j.1365-3091.1994.tb02013.x.

Zijlstra H.J., 1987. Early diagenetic silica precipitation, in relation to redox boundaries and bacterial metabolism, in Late Cretaceous chalk of the Maastrichtian type locality. *Geologie en Mijnbouw*, 66, 343–355.